Further Development of a Barotropic Operational Model for Predicting Paths of Tropical Storms

FREDERICK SANDERS, ALAN L. ADAMS,[1] NORMA J. B. GORDON[2] AND WADE D. JENSEN[3]

Department of Meteorology, Massachusetts Institute of Technology, Cambridge 02139

(Manuscript received 6 August 1979, in final form 11 January 1980)

ABSTRACT

To enable use of aircraft winds and satellite cloud-motion vectors in the SANBAR model for prediction of tropical storm tracks, we have derived regression equations for estimating the tropospherically averaged flow from information at one, two or three levels. Two-level results represent an improvement over climatology and a third level yields substantial further improvement. We find from a study of the 1975 season in the Atlantic Basin that reduction in initial position and track-velocity errors can produce substantial improvement in position-forecast accuracy out to 72 h range. We recommend a new procedure for evaluating and using wind observations within the region influenced by the storm circulation. The new method has the potential for substantial reduction of present forecast error for storms within 24 h of landfall.

1. Introduction

A barotropic filtered model (SANBAR) was developed by Sanders *et al.* (1975) and by others for operational prediction of the tracks of tropical storms at ranges out to 72 h. This model has been used since 1968 at the National Hurricane Center (NHC), where recent results (see Table 1)[4] indicate that it performs competitively with other objective models which are credited (Dunn *et al.*, 1968) for the improvement, however slow, in the final subjective judgement.

We were prompted to try barotropic prediction because its basic mechanism, the conservation of absolute vorticity, is an explanation of the apparent "steering" of the intense storm vortex by the larger scale current in which it is embedded, as suggested by Riehl *et al.* (1956) and by Jordan (1952), among others before and since. On physical grounds, too, it seemed that variation of vorticity advection across the storm center was the most likely effect in the vorticity equation for producing storm motion. We say this because the more intense the vorticity maximum, the more intense the cross-center gradient of the mechanism must be to produce a given motion of the center. The cross-center gradient of horizontal advection becomes more intense as more intense vorticity maxima are considered. It seems unlikely that non-advective effects, principally convergence and divergence, can produce dominant effects on storm motion, in view of the typically symmetric character of the cloud and precipitation near the center, unless the large-scale steering is extremely weak. Baroclinic effects, of course, may play an important role in the temporal evolution of the large-scale motions themselves, which will have an important effect on storm motion beyond the shortest ranges, but it seemed desireable to exploit the relatively inexpensive barotropic calculation as a first step.

The failure of earlier attempts at barotropic prediction (e.g., Birchfield, 1960; Vanderman, 1962; Kasahara, 1959) to achieve operational acceptance was regarded as due to the difficulty of establishing an adequate initial large-scale analysis on the basis of rawinsonde-derived pressure data in lower latitudes, where errors are often as large as natural variability. Hence the SANBAR model relies on an analysis of wind observations, averaged through the depth of the troposphere, and makes no direct reference to the pressure-height data. Difficulties with the separation of the vortex from the large-scale flow in the *forecasting* process (Kasahara, 1959), led us to utilize a relatively small 150 km mesh length and to *predict* the storm as an integral part of the total flow field.

Two problems had to be dealt with immediately: 1) analysis over the tropical oceans where rawinsonde data are almost completely absent, and 2) assessment of the effect of the storm circulation, as distinct from the large-scale influence, on soundings made in the vicinity of the storm (necessary for

[1] Air Weather Service, U.S. Air Force.

[2] Bureau of Air Quality Control, Maine Department of Environmental Protection, Augusta, ME.

[3] Meteorology Research, Inc., Altadena, CA.

[4] From C. J. Neumann, 1979: A guide to Atlantic and Eastern Pacific Models for the prediction of tropical cyclone motion. NOAA Tech. Memo. NWS NHC-11. [NTIS $$$ $$$]. The other models are discussed therein.

0027-0644/80/050642-13$07.25

© 1980 American Meteorological Society

TABLE 1. Homogeneous sample of forecast position errors (n mi) over period 1973–78 in the Atlantic Basin.

Model	Range			
	12 h	24 h	48 h	72 h
CLIPER	56	125	276	381
NHC 67	56	119	293	428
NHC 72	55	120	269	393
NHC 73	54	120	244	367
SANBAR	60	121	256	389
Number of cases	261	232	161	109

realistic construction of the total initial flow). The first was handled by the provision, at first subjectively and later by objective automated means (Pike, 1975, private communication), of "bogus" wind data at a coarse array of points covering large portions of the SANBAR forecast area. The second problem was first handled by subtracting from nearby wind observations a vector contribution from an idealized axisymmetric vortex specified by the geographical position of its center, and by its maximum wind, eye diameter and radius of influence. All of these parameters except the last are reasonably well known initially in real time. The radius of influence was subjectively determined, with results that often seemed so unsatisfactory that 300 n mi was adopted as an almost ubiquitous nominal value. When this technique continued to provide unreasonable-looking "residual" large-scale winds from time to time, it was decided to ignore nearby wind soundings altogether and to substitute, at the affected points of the SANBAR grid, first (Pike, 1972) the vector sum of the storm contribution described above and a constant large-scale contribution equal to the recently observed direction and speed of the storm track, and later (Sanders *et al.*, 1975) a fixed streamfunction field calculated from these winds and the storm parameters.

Aside from purely technical improvements in the SANBAR calculations two avenues seem open for improving performance. One stems from the improvement in the large-scale oceanic data base over the past decade, due to increased numbers of better wind observations from aircraft and especially to large numbers of wind estimates now derived from cloud motions observed by geosynchronous satellites. The other road to improvement, however difficult it has been in the past, must lie in the effective use of wind observations in the storm-influenced region. This paper reports principally our efforts along these two lines.

2. Regression estimates of the tropospheric mean wind

The current data base over the oceans comprises relatively dense coverage in the lowest 2 km, from surface observations by ship and from low cloud-motion observations by satellite, and in the layer from 9 to 12 km, from wind observations derived from aircraft navigation systems and from high cloud motions observed by satellite. We must infer the tropospheric mean wind from information in these two layers.

Thus, following preliminary work by Pike (1975, private communication), we derived some definitive regression equations from an extensive sample of data in the NHC region of forecast responsibility during the period June–October 1971–74. In these equations rawinsonde wind observations at 850 and 250 mb were used to approximate the tropospheric mean wind calculated from the winds at the 10 mandatory pressure levels from 1000 to 100 mb in the same soundings. Our results, obtained from a total of 11 682 observations in June–October at Bermuda, San Juan, Hatteras, Miami, Tampa, Lake Charles, Brownsville and Merida, are given in Table 2.

Note that the root-mean square error, if not reduced by the analysis and initialization processes, would yield 24 h rms displacement errors of 82 and 74 n mi in the zonal and meridional directions, respectively. These errors would be larger when available surface, aircraft and satellite observations are used in regression equations tailored for rawinsonde data. In fact, these errors approach present state-of-the-art errors, so that we cannot expect use of our two-level regression equations to improve dramatically the statistics of forecast errors. We might hope, nevertheless, that their use would reduce the number of very large errors made far from the reach of rawinsonde data when the initial analysis relies on less systematic application of the few available data.

In the anticipation that SANBAR might be used in other regions of the Northern Hemisphere, we obtained similar equations for the eastern Pacific (from 5594 observations at Vandenberg, AFB, Hilo, Johnston Island and Midway Island), and for the western Pacific (from 10 145 observations from Guam, Wake Island, Truk, Ponape, Kwajalein, Majuro, Yap and Koror).[5] Equations for these two

[5] The former of these sets may not represent the wind structure in the zone of tropical cyclogenesis, where next to no rawinsonde data exist, but they should be more reliable as the storm approaches these populated locations.

TABLE 2. Regression equations for estimated zonal and meridional components of tropospherically averaged winds, in NHC region of responsibility. Speeds are in knots.

	Reduction of variance	Root-mean square error
$\hat{u}_{1000-100\text{ mb}} = +0.4 + 0.53u_{850} + 0.37u_{250}$	0.92	3.4
$\hat{v}_{1000-100\text{ mb}} = -0.5 + 0.45v_{850} + 0.33v_{250}$	0.85	3.1

TABLE 3. Regression equations for eastern and western Pacific regions. Speeds are in knots.

	Reduction of variance	Root-mean square error
Eastern Pacific		
$\hat{u}_{1000-100\text{ mb}} = +0.2 + 0.52u_{850} + 0.36u_{250}$	0.87	3.9
$\hat{v}_{1000-100\text{ mb}} = +0.1 + 0.46v_{850} + 0.36v_{250}$	0.88	3.3
Western Pacific		
$\hat{u}_{1000-100\text{ mb}} = -2.2 + 0.43u_{850} + 0.32u_{250}$	0.77	3.3
$\hat{v}_{1000-100\text{ mb}} = -0.4 + 0.40v_{850} + 0.26v_{250}$	0.70	2.7

additional regions are given in Table 3. The results indicate no substantial difference between the Atlantic and eastern Pacific areas. In the western Pacific, however, the zonal equation is quite different, and it appears that the vertical structure of the zonal component is noisier. Although the reduction of variance in both components is smaller in this region, so is the rms error, indicating that the wind is less variable in the Pacific sample, but we cannot tell to what extent the reduction is temporal or spatial.

Stratification of the above samples into early-season (June–August) and late-season (September–October) portions showed only minor differences in the resulting regression equations, reductions of variance and rms errors.

The accuracy of estimate of the tropospheric-mean wind, however, is sensitive to the number of levels at which information is available. We derived regression equations appropriate for the unfortunate circumstances when only low-level or only high-level data were available, and for the optimistic hope that wind information for a mid-tropospheric level (say, 500 mb) might somehow become available. These equations are shown in Tables 4 and 5 in which the data of Table 1 are included for comparison. If only one level is available, the mean wind can probably be specified with little or no skill relative to local climatology, although one is somewhat better off to have data in the upper than in the lower troposphere. If the middle tropospheric data could be added to observations at the other two levels, substantial improvement would be felt in specification of the tropospheric mean wind. Comparing Tables 4 and 5, we see large differences when data are available at only one level, because of the different vertical structure of wind fields in the two regions; but when data are available at three levels the regression equations and the rms errors are almost identical.

The reductions of variance suggest more skill than is actually present in the equations, because part of the variance doubtless resides in differences in the climatological average wind from station to station within each region. This is particularly true of the sample from the Atlantic sector.

We made no attempt to use zonal components as predictors for meridional components of the tropospheric mean winds or vice versa. Such an attempt might yield useful results if trough and ridge tilts, for example, were consistently northeast–southwest or northwest–southeast, but substantial improvement over what we have already obtained seems unlikely.

When satellite cloud-motion vectors are used in place of rawinsonde data in the two-level equations (as would be done in practice, for example) we estimate a 50% increase in the rms error of specification of the tropospheric-mean wind. The details of this estimation, and of the entire regression analysis, are given by Adams and Sanders (1975).

3. Sources of error in 1975 operational forecasts

We undertook to study the causes of large SANBAR forecast errors in the 1975 hurricane season, with the aim of applying our regression equations

TABLE 4. Regression equations for one, two and three levels of information for region of NHC forecast responsibility. Speeds are in knots.

	Reduction of variance	Root-mean-square error
One level		
$\hat{u}_{1000-100}(850) = +4.8 + 0.71u_{850}$	0.43	8.8
$\hat{u}_{1000-100}(250) = -2.1 + 0.43u_{250}$	0.69	6.5
$\hat{v}_{1000-100}(850) = -1.5 + 0.51v_{850}$	0.34	6.6
$\hat{v}_{1000-100}(250) = +0.9 + 0.35v_{250}$	0.60	5.2
Two levels		
$\hat{u}_{1000-100}(850, 250) = +0.4 + 0.53u_{850} + 0.37u_{250}$	0.92	3.4
$\hat{v}_{1000-100}(850, 250) = -0.5 + 0.45v_{850} + 0.33v_{250}$	0.85	3.2
Three levels		
$\hat{u}_{1000-100}(850, 500, 250) = -0.1 + 0.31u_{850} + 0.36u_{500} + 0.26u_{250}$	0.97	1.9
$\hat{v}_{1000-100}(850, 500, 250) = -0.3 + 0.30v_{850} + 0.35v_{500} + 0.24v_{250}$	0.95	1.8

TABLE 5. Regression equations for one, two and three levels of information for the western Pacific region. Speeds are in knots.

	Reduction of variance	Root-mean-square errors
One level		
$\hat{u}_{1000-100}(850) = -4.5 + 0.28u_{850}$	0.24	6.0
$\hat{u}_{1000-100}(250) = -5.9 + 0.22u_{250}$	0.28	5.8
$\hat{v}_{1000-100}(850) = -0.8 + 0.40v_{850}$	0.24	4.3
$\hat{v}_{1000-100}(250) = +0.2 + 0.26v_{850}$	0.42	3.7
Two levels		
$\hat{u}_{1000-100}(850, 250) = -2.2 + 0.43u_{850} + 0.32u_{250}$	0.77	3.3
$\hat{v}_{1000-100}(850, 250) = -0.4 + 0.40v_{850} + 0.26v_{250}$	0.70	2.7
Three levels		
$\hat{u}_{1000-100}(850, 500, 250) = -0.8 + 0.28u_{850} + 0.32u_{500} + 0.25u_{250}$	0.92	1.9
$\hat{v}_{1000-100}(850, 500, 250) = -0.4 + 0.30v_{850} + 0.31v_{500} + 0.24v_{250}$	0.89	1.7

in revised predictions. As a preamble to this effort, we made revised forecasts based on post-season "best-track" initial positions and track velocities (Hebert, 1976). As illustrated in Table 6, these revised forecasts presented a substantial improvement over the original operational predictions at ranges out to 48 h. On the other hand, the mean initial errors in position and track velocity (based on the premise that the best-track information represents absolute truth) suggest that it will be extremely difficult to reduce the mean SANBAR position error in the 24 h forecast below 75 n mi, the expected (or hoped for) error cited by Sanders and Burpee (1968).

Incidentally, the 1975 tracks were remarkable in two respects: only one storm failed to recurve toward the northeast, and no storm executed a loop or other exotic excursion. There was a slight tendency for operational positions to lie westward of the best-track locations and for operational track velocities to be insufficiently northeastward, both biases probably due to the forecasters' reluctance to anticipate fully the degree of recurvature and acceleration which was actually occurring. In the event of erratic storm tracks, operational errors in initial position and track velocity would probably have been larger.

Sanders and Gordon (1976) studied a number of the 1975 cases in detail, finding the large forecast errors to stem from a variety of causes. One of the cases analyzed in detail, for Faye starting at 0000 GMT 26 September, is illustrated in Figs. 1 and 2. From a comparison of predicted and observed tracks in Fig. 1, it is seen first that the slow predicted speed was responsible for the large 212 n mi operational error at 24 h, which was improved in the best-track prediction only by a more accurate specification of the initial track direction. Second, neither forecast anticipated the dramatic acceleration after 48 h, producing errors of 961 and 772 n mi in the operational and best-track predictions at 72 h.

The unusually dense initial observational coverage shown in Fig. 2, comprising mainly wind estimates from satellite-observed cloud-motion vectors, precludes lack of data as an explanation of the forecast errors. It appears, however, that the numerous observations within the 300 n mi influence distance of Faye indicate a large-scale flow toward the northwest at a speed in excess of the specified initial speed. Application of the regression equations in Table 1 indicates, in fact, a large-scale speed of about 15 kt, in contrast to the initial 11 kt specified initially in both the operational and best-track predictions. The 12 h observed displacement speed was in fact 17 kt. In the present analysis procedure, of course, these wind data are discarded in favor of the specified initial speed. Clearly, useful data are being lost.

The large error at 72 h arises from another cause. Fig. 3 shows the initial large-scale flow pattern, with its observed and predicted change. The ridge which

TABLE 6. Comparison of operational and best-track forecasts.

	00 h	12 h	24 h	36 h	48 h	72 h
Mean position error, operational forecasts (n mi)	15	67	121	181	261	393
Mean position error, best-track forecasts (n mi)	0	50	99	152	224	376
Percentage improvement of best-track over operational forecasts	100	25	18	16	14	4
Mean magnitude of error in operational specification of initial track velocity (kt)	2.8	—	—	—	—	—
Number of forecasts	74	67	58	51	44	33

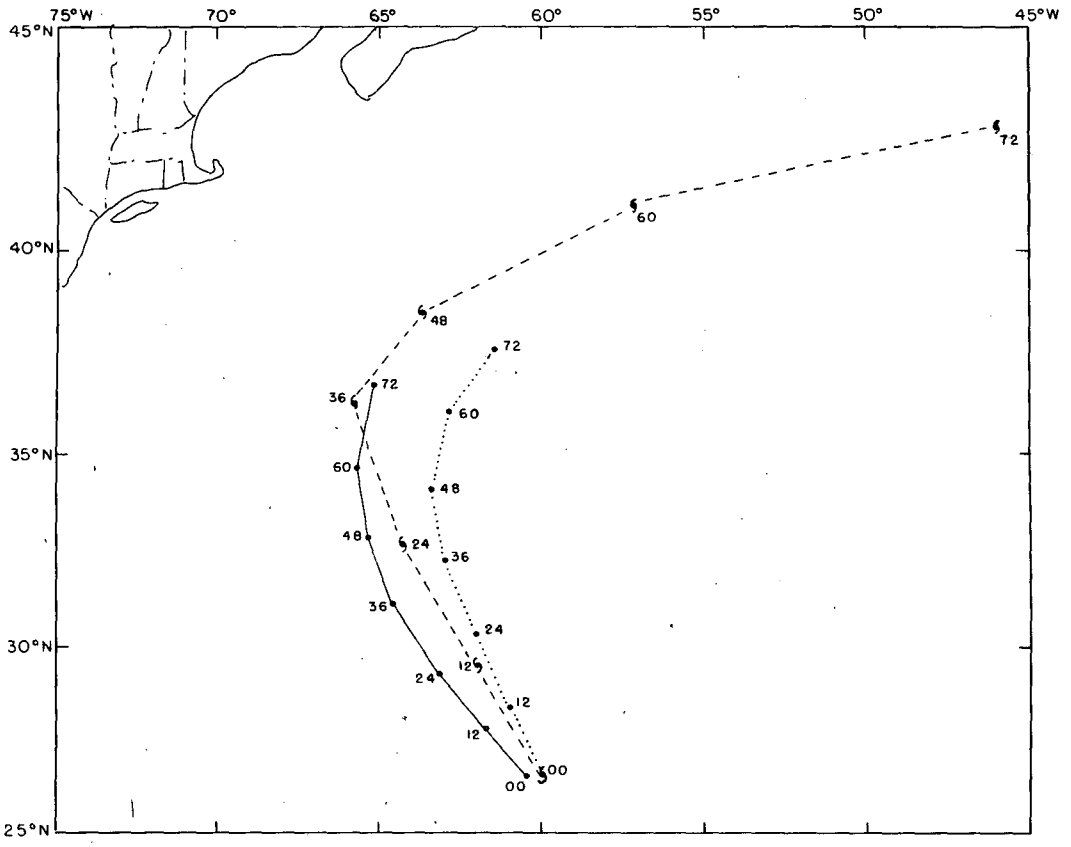

FIG. 1. Tracks of Faye 0000 GMT 26 September. Dashed line indicates observed track, solid line operational forecast track, and dotted line best-track revised forecast. Dots show forecast positions, labeled in number of hours after initial time. Corresponding observed positions are shown by hurricane symbols.

initially extended northwestward of the storm was predicted to change little during 48 h, whereas, in fact, the trough in the central United States advanced northeastward to pick up the accelerating storm. The forecast error was evidently not due to fixed boundary conditions in the SANBAR model but rather to the presence of important baroclinic effects. This view is supported by the portions of the National Meteorological Center hemispheric 500 mb prognostic charts shown in Fig. 4. Note that the barotropic forecast suffers from the same defect as the SANBAR prognosis, while the baroclinic PE forecast has the right idea, as usual, but is a bit slow about it. Note further from Fig. 2 that the large-scale structure in the vicinity of the storm was hardly barotropic. The tropospheric shear in this case was substantial and well organized, with a probable direct effect on storm behavior.

In other instances, large SANBAR forecast errors were found to be attributable to failure to use satellite-derived pressure-height data poleward of 30°N, to paucity of data of all types, and to fixed values of vorticity and streamfunction on the northern boundaries of the grid area.

4. Interpretation of storm-influenced winds

Rawinsonde observations made within the circulation of a tropical storm, often with great difficulty and at substantial hazard to the observers, should be a valuable source of information concerning the track of the storm. Yet both the SANBAR and MFM (Hovermale, 1975) models discard all such observations. The reason, in the case of SANBAR, is that we have not been able objectively to evaluate the contribution of the storm circulation with sufficient accuracy.

The idealized radial profile of the tangential storm wind component used operationally in SANBAR (Sanders *et al.*, 1975) is given by

$$V_\theta = 0.72V_{\max} \times \left\{\sin\left[\pi\left(\frac{R}{R_{\max}}\right)^{\log 0.5/\log(R_{\text{eye}}/R_{\max})}\right]\right\}^{1.5}, \quad (1)$$

where $V_{\max}$ is understood to be the maximum surface wind (kt) as given in the current advisory, R_{eye} is the radial distance from the center of the eye to the maximum wind (nearly always taken as 20 n mi), and $R_{\max}$ is the maximum influence distance of the

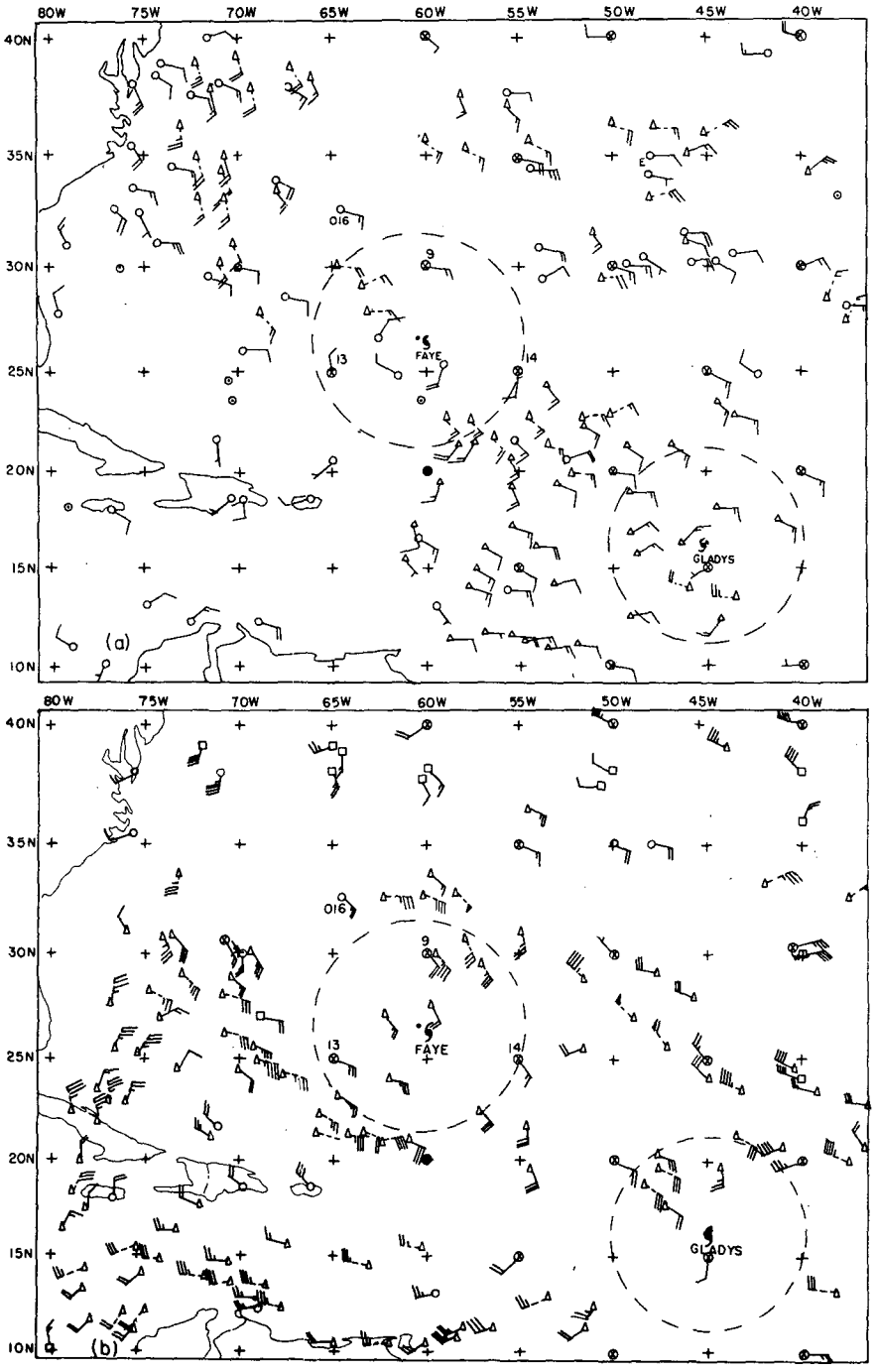

FIG. 2. Data bases for oceanic analysis 0000 GMT 26 September: (a) near surface, (b) 200 mb level. Positions of bogus points are shown by ⊗'s. Radius of influence is shown by the dashed circle. Dashed arrows indicate data not received by operational deadline time.

storm (nearly always taken as 300 n mi). This expression can be written as

$$V_\theta = X_1\left\{\sin\left[\pi\left(\frac{R}{300}\right)^{X_2}\right]\right\}^{X_3}. \qquad (2)$$

We have considered the possibility of allowing the wind observations within the storm-influenced region to tell us the "best" values of the storm parameters X_1, X_2, X_3, rather than using a profile prescribed without examination of the observations, a practice which often yields unrealistic and irregular residual winds. By best we mean those values of the

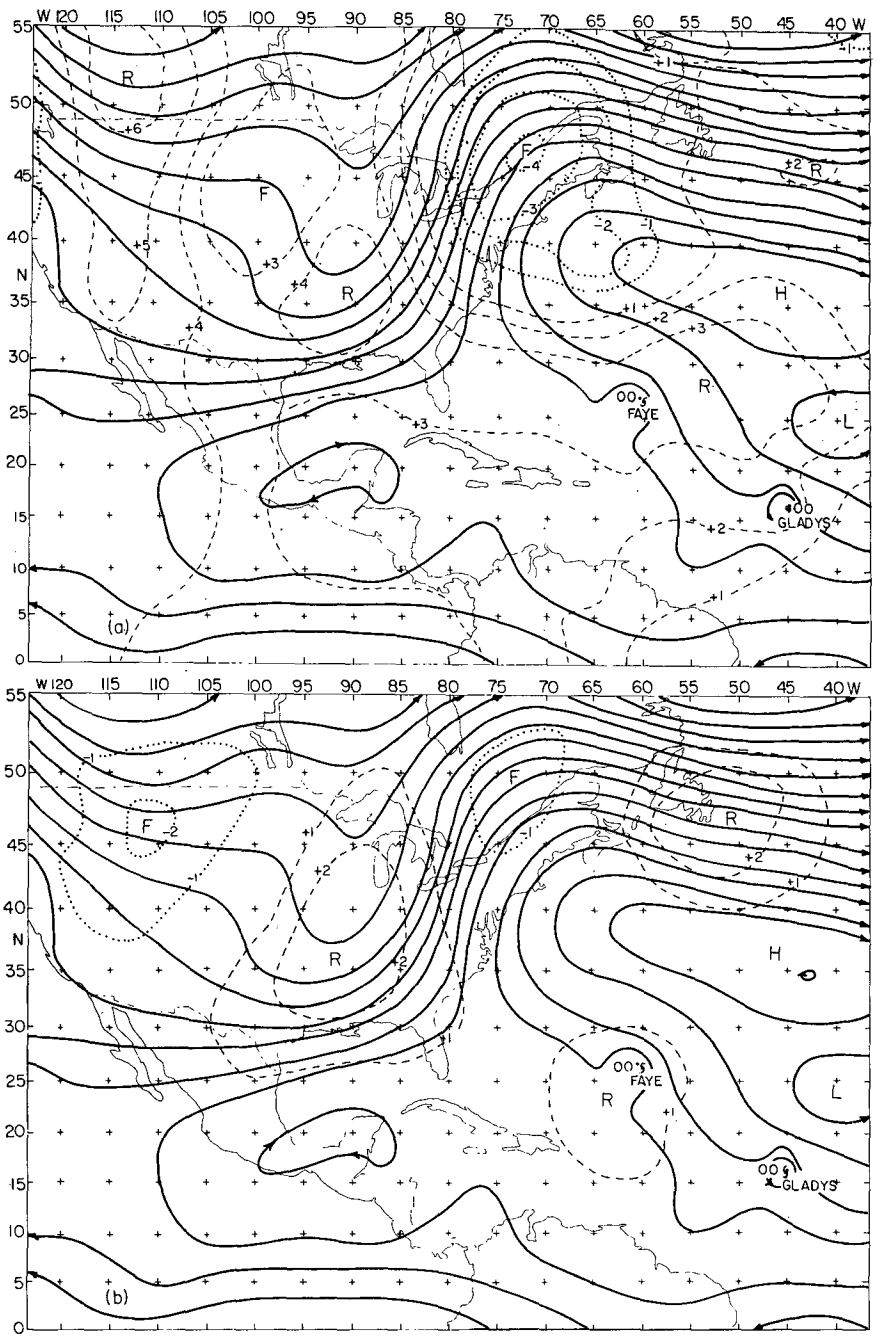

FIG. 3. Large-scale initial flow pattern 0000 GMT 26 September (solid lines) and 48 h streamfunction changes for (a) observed and (b) predicted by SANBAR. Streamfunction lines are at intervals of 3×10^6 m^3 s^{-2}. Dashed lines indicate streamfunction rises and dotted lines falls, in units of 3×10^6 m^3 s^{-2}.

parameters that yield the "smoothest" set of residual winds V_r, given by

$$\mathbf{V}_r(X_1,X_2,X_3) \equiv \mathbf{V}_o - \mathbf{V}_\theta(X_1,X_2,X_3),$$

where $\mathbf{V}_o$ is the observed wind. By smoothest we mean a set of residual winds that shows the closest fit to a linear interpolation among the winds at the three stations surrounding each station in the influence region. Specifically, consider station A surrounded by stations B, C and D, as illustrated in Fig. 5. Observed winds are shown for stations B and C. At station D a residual wind is shown because it is within the maximum influence distance of the tropical storm. Bilinear interpolation of the zonal

and meridional components yields a plane-fit wind $\mathbf{V}_p$ at station A. The difference $\mathbf{V}' \equiv \mathbf{V}_r - \mathbf{V}_p$ at station A is a measure of the smoothness of that value of $\mathbf{V}_r(X_1,X_2,X_3)$. We chose as the optimum values of X_1, X_2, and X_3 for a given synoptic case that set, from the possibilities given in Table 7, which minimized the rms magnitude of $\mathbf{V}'$ over the stations within the maximum influence distance for that case.

Finally, of course, the values of $\mathbf{V}_r$ should provide a good specification of the storm-track velocity at the time of the observations. We would hope that this specification is as accurate as the operational estimate made in real time by NHC for the official advisories. To this end, a value of $\mathbf{V}_r$ at the location of the storm center was determined, for the optimum set of storm parameters, by stepwise screening regression for both zonal and meridional wind components, given the station values of $\mathbf{V}_r$. We would be satisfied if initial specification of storm-track velocity were as accurate as operational estimation, because our proposed procedure yields a variable large-scale wind field in the vicinity of the storm, with the possibility of substantial predicted changes in track velocity, whereas the current operational procedure yields a displacement in the first 12 h at very nearly the instantaneous initial velocity.

Fifty data sets, for nine tropical storms, were

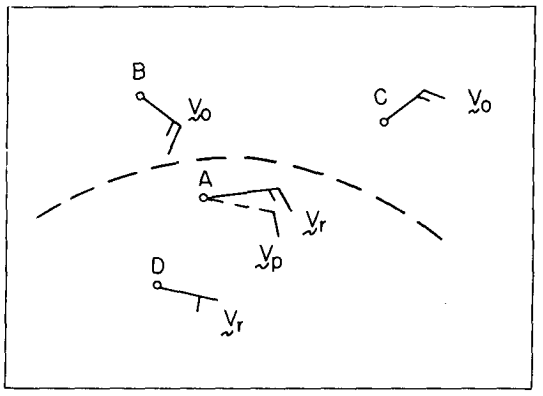

FIG. 5. Illustrating a comparison between the residual wind at station A and the plane-fit wind, $\mathbf{V}_p$, obtained by interpolation between observations at stations B, C and D.

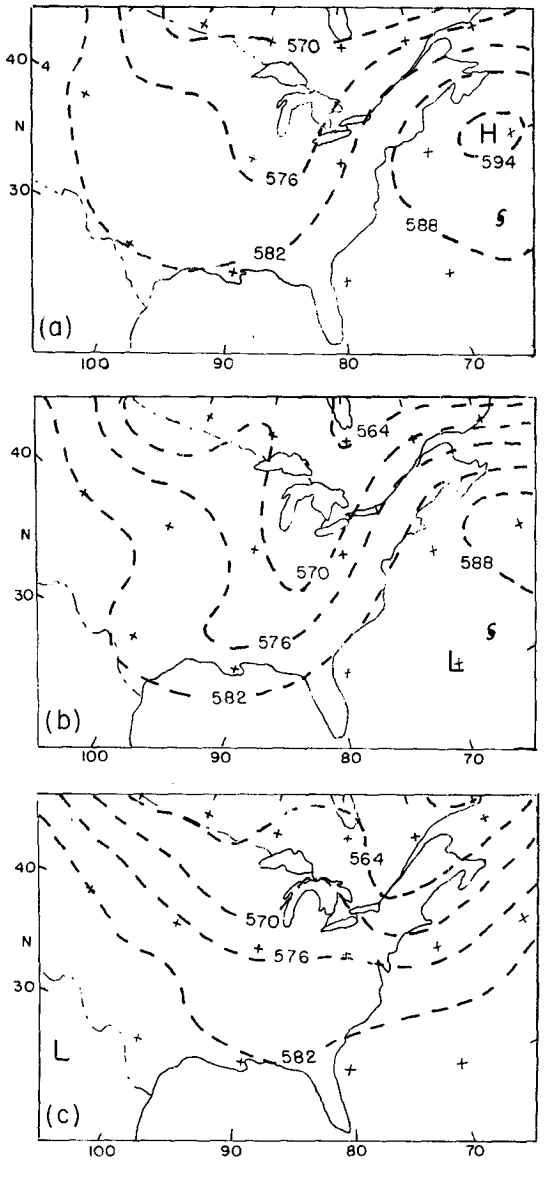

FIG. 4. NMC prognostic charts: (a) 36 h barotropic forecast valid at 0000 GMT 27 September; (b) 24 h PE baroclinic forecast valid at 0000 GMT 27 September; and (c) 72 h PE forecast valid at 0000 GMT 29 September.

TABLE 7. Frequency of values of parameters chosen to minimize V':

$$X_1 = 0.72V_{\max}, \quad X_2 = \frac{\ln 0.5}{\ln(r_e/300)}.$$

X_1 (kt)	N	r_e (n mi)	N	X_3	N
5	0	3	7	0.2	13
10	8	6	1	0.4	5
15	6	9	5	0.6	3
20	7	12	4	0.8	6
25	4	15	7	1.0	2
30	1	18	1	1.2	6
35	4	21	2	1.4	5
40	2	24	2	1.6	2
45	3	27	2	1.8	2
50	0	30	2	2.0	1
55	0	33	2	2.2	0
60	0	36	1	2.4	0
65	1	39	2	2.6	1
70	2	42	1	2.8	0
75	3	45	1	3.0	2
80	0	48	2	3.2	1
85	2	51	1	3.4	0
90	5	54	1	3.6	0
95	2	57	1	3.8	0
100	0	60	5	4.0	1
Total	50		50		50

TABLE 8. Frequency of errors of specification of initial track velocity and of 12 h extrapolation forecast based on it.

Error range (kt) Initial track velocity	Frequency	Error range (n mi) 12 h forecast position	Frequency
0–1.7	7	0–20	5
1.8–3.3	9	21–40	11
3.4–5.0	14	41–60	16
5.1–6.7	11	61–80	8
6.8–8.3	4	81–100	3
8.4–10	3	101–120	3
>10	2	>120	4
Total	50		50

chosen for study on the basis of the presence of two or more simultaneous rawinsonde observations within the influence region of the storm. Understandably, these storms lay within 300 n mi or so of the United States coast and thus represented especially important forecast problems for NHC. Selection frequencies for the discrete values of X_1, X_2 and X_3 are shown in Table 7. We note with surprise that in about half the instances the implied value of V_{max} is no more than 35 kt, and that the shape of the radial profile is very flat, as evidenced by small values of X_3. The current operational SANBAR value of $X_3 = 1.5$ is exceeded less than 20% of the time in the present sample. Study of individual cases shows that the tropical storm is often em-

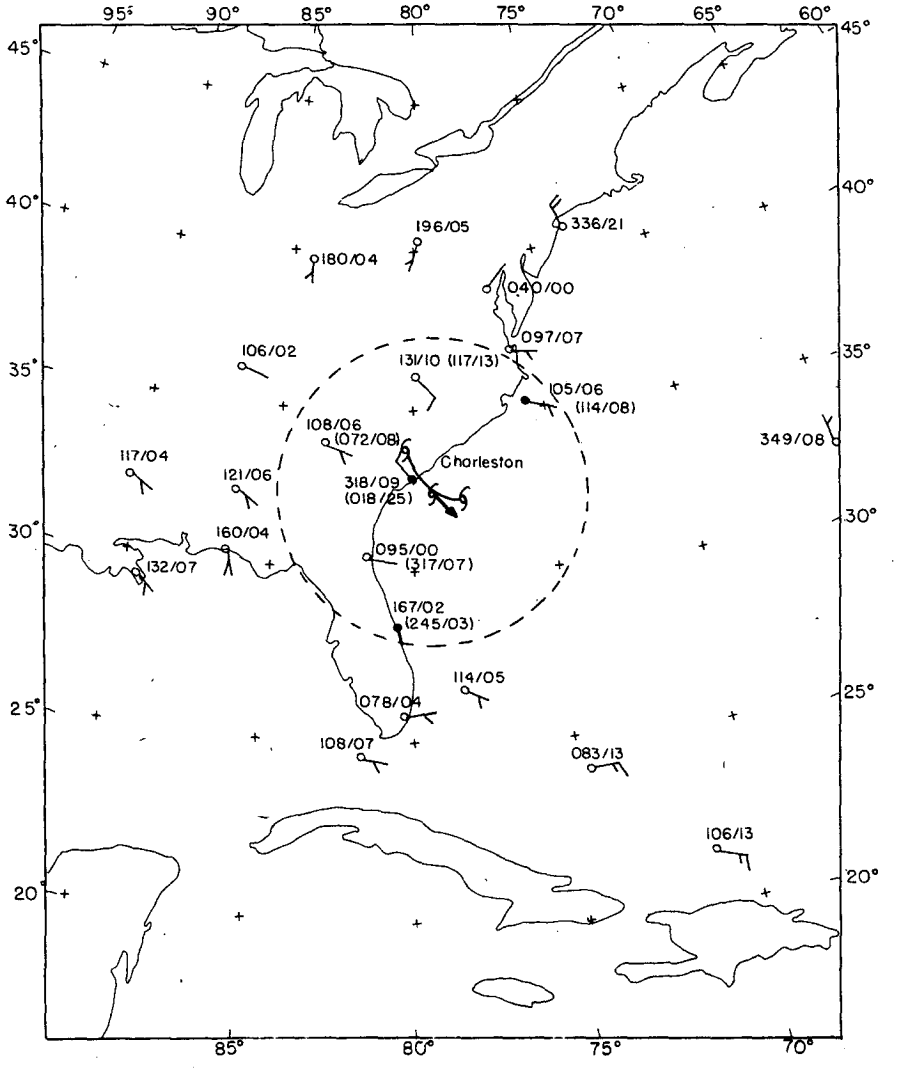

FIG. 6. Initial mean winds for 0000 GMT 9 July 1959. Central position and influence region of Hurricane Cindy are shown, respectively, by the hurricane symbol and the dashed circle. Positions of the storm 12 h earlier and later are shown by hurricane symbols southeast and northwest, respectively, of the current position. The length and direction of the heavy arrow represent a 12 h linear displacement at the specified velocity. Plotted winds represent V_r, also given by numerical notation. Values in the parentheses denote the observed wind V_0.

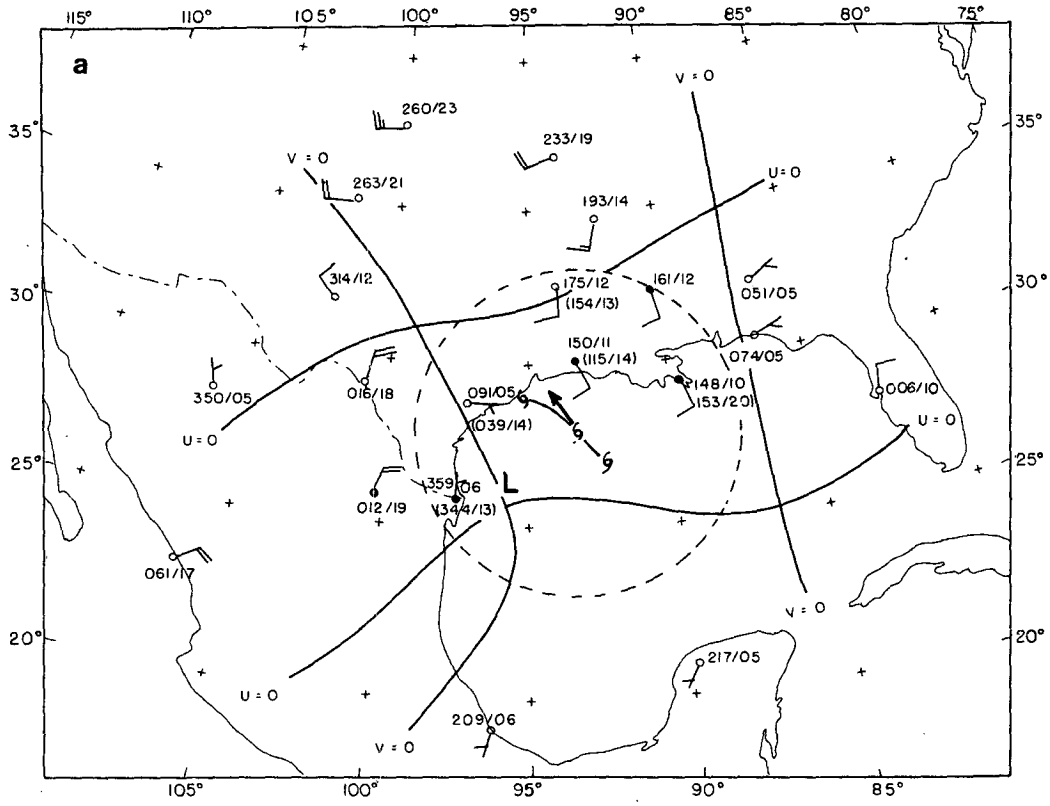

FIG. 7a. Initial mean winds for Hurricane Delia, 1200 GMT 4 September 1973. Notation as in Fig. 6, except that heavy lines represent zero isopleths for zonal and meridional velocity components.

bedded in a relatively weak cyclonic circulation of relatively large scale, and that really strong winds are rarely sampled by the rawinsonde system, leading to these unexpected results.

For each synoptic case, we compared the specified initial track velocity emerging from the regression analysis with an estimate of the actual initial velocity obtained from the best-track information. The mean magnitude of the vector difference was 4.2 kt, slightly worse than the probable discrepancy between operationally specified and best-track initial velocities, as discussed earlier. The frequency distribution of the differences in Table 8 shows, however, that operational accuracy was probably exceeded about half the time, and that our regression procedure occasionally yielded extremely large errors. Examination of cases showed that these tended to be instances in which rawinsonde observations were available in only a single quadrant of the storm. There was little bias in specified direction or speed. A deficiency in westward motion might be expected due to our neglect of the effects of the latitudinal variation of earth vorticity, but the effect is evidently small enough to be masked by other sources of error.

In a few cases in which the storm center was very close to a sounding location the regression result was extremely sensitive to the position of the center and large errors were likely. Ten cases of this type were recalculated with the station less than 85 n mi of the center excluded, yielding much improved results. Fig. 6 shows such a case, in which the error is 13 kt, between the specified southeastward and the observed northwestward motion. If the storm center were located 17 n mi to the north-northeast, however, and the storm wind contribution to the Charleston observation were increased from 22 to 28 kt, then a perfect specification would have resulted. Modest asymmetry in the storm circulation as well as moderate position error could produce the large specification error.[6] Thus, we are still unable to make constructive use of observations very close to the storm center.

An especially interesting storm is Delia 1973, which performed a loop along the Texas Gulf Coast before moving inland. The operational SANBAR 24 h forecasts were very poor during this time, for obvious reasons. The numerous observations within the influence region were discarded in favor of a straight uniform large-scale flow representing the most recent storm-track vector. Our new procedure,

[6] A recalculation with the Charleston observation excluded yielded an error of 3 kt.

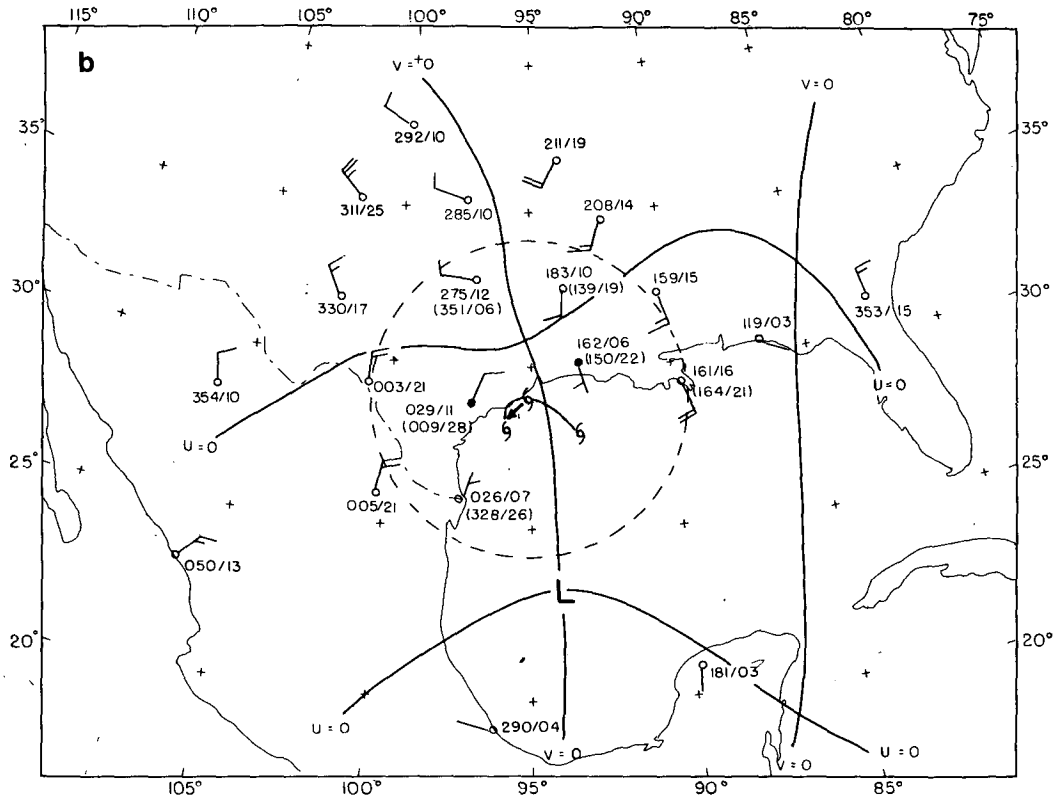

FIG. 7b. Initial mean winds for Hurricane Delia, 0000 GMT 5 September 1973. Notation as in Fig. 6.

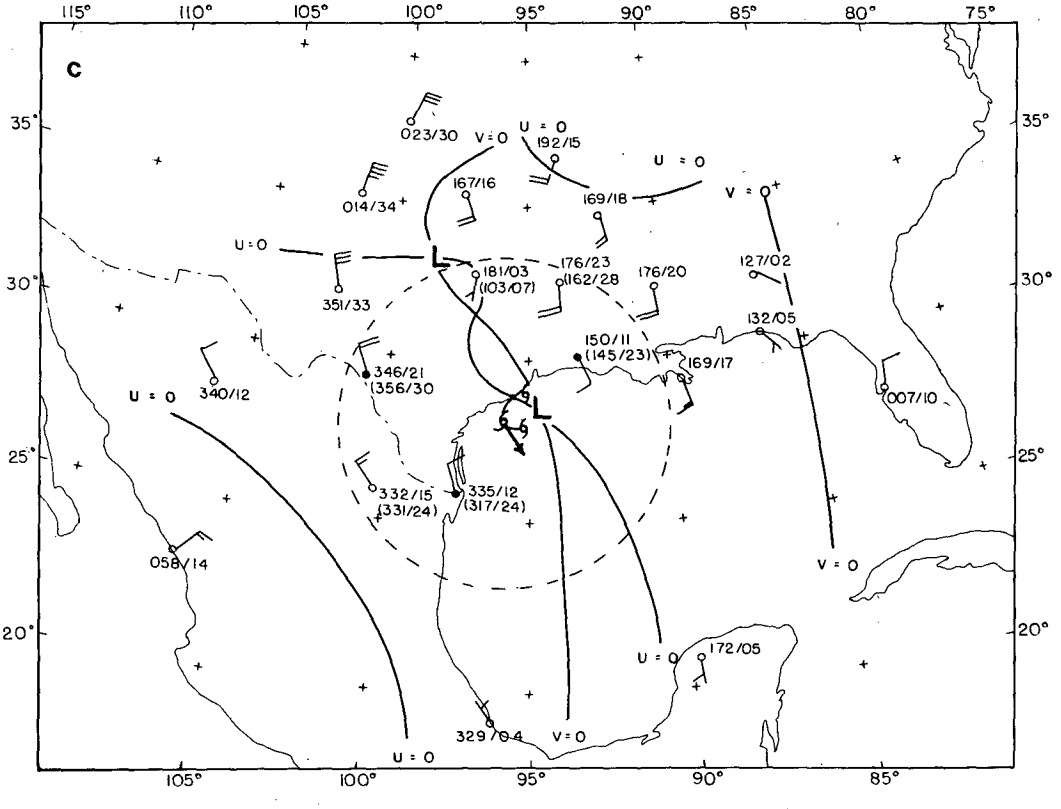

FIG. 7c. As in Fig. 7b except for 1200 GMT 5 September.

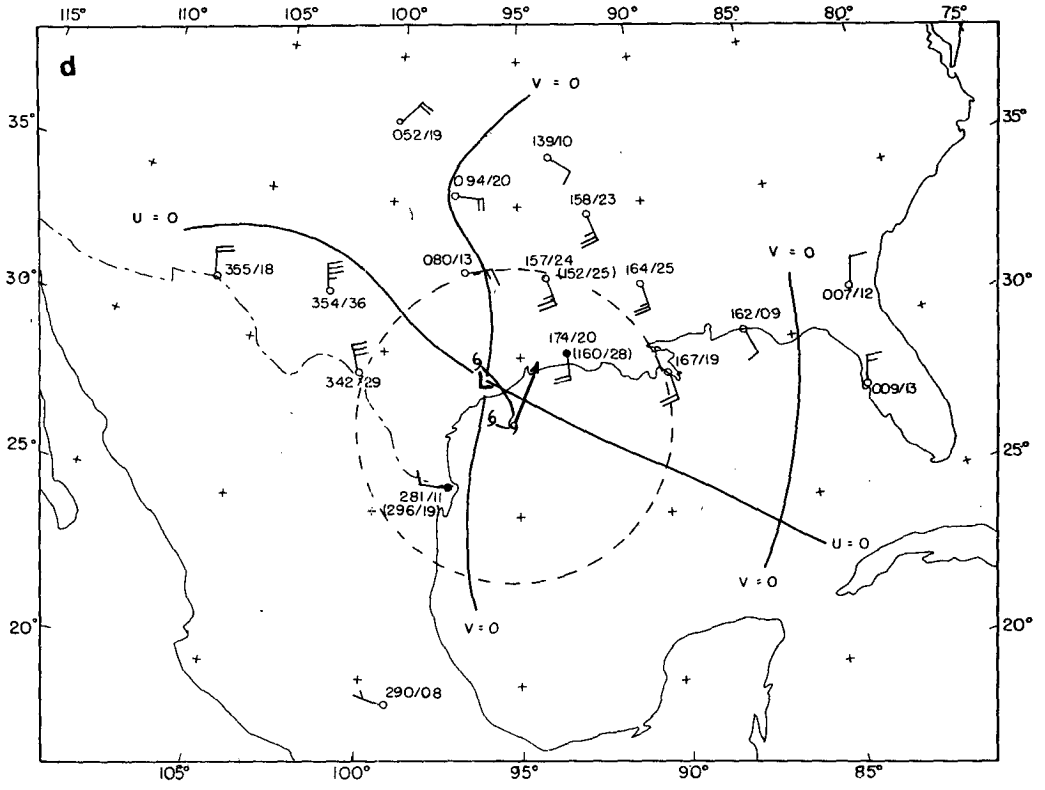

FIG. 7d. As in Fig. 7b except for 0000 GMT 6 September.

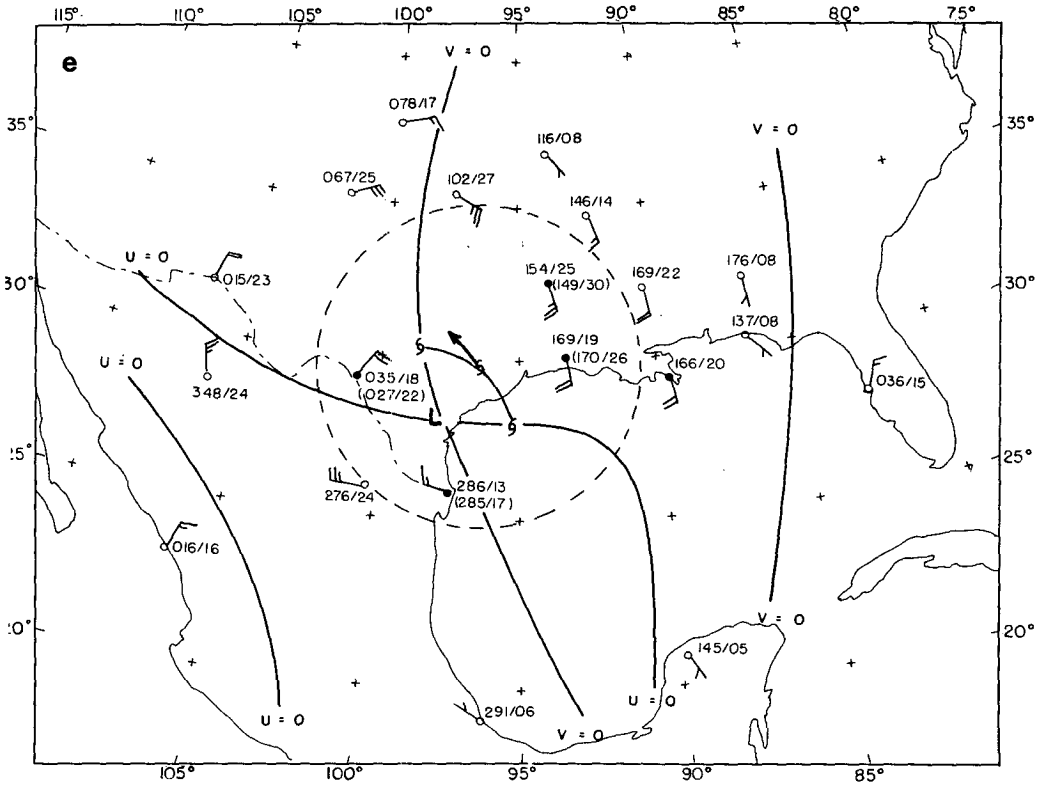

FIG. 7e. As in Fig. 7b except for 1200 GMT 6 September.

as illustrated in Fig. 7, shows excellent specification of the track velocity during the loop (probably better than the velocity estimated in real time), as Delia and a larger cyclone, denoted by the heavy block letter, circle about each other. The looping motion of Delia seems plainly accountable as a barotropic process. The motion of the larger cyclone is a moot question.

Although the new procedure has not been incorporated in the SANBAR analysis program, we estimated the errors that would have ensued from using the specified track velocity as a 12 h extrapolation forecast. The frequency of various ranges of error in this forecast is given in Table 8. Despite the presence of some large errors in this sample, the primary potential advantage of the new procedure is that the large-scale flow in the storm-influenced region is not constrained to be uniform.

5. Concluding Summary

For use of aircraft winds and satellite cloud-motion vectors in the SANBAR prediction model, we have derived some definitive regression formulas, for the zonal and meridional components of the wind averaged over the depth of the tropical troposphere, given 1) data in the lower or upper troposphere alone, 2) in both these layers, and 3) in the middle troposphere as well as in these layers. We find that data at only one level yield a result little better than use of the climatological mean, while addition of middle-tropospheric data, difficult with current satellite capability, would improve substantially upon estimates based on lower- and upper-tropospheric data. We find some benefit in use of separate formulas for the Atlantic and Pacific areas, but little in stratification into earlier and later portions of the tropical-storm season.

From a study of SANBAR forecast errors, we find that the present model suffers from inaccurate specifications within the storm-influenced region, from neglect of pressure-height data outside the tropics, from fixed boundary conditions in the middle-latitude portion of the forecast grid, and from neglect of baroclinic effects in the large-scale flow pattern surrounding the storm.

We recommend a new procedure for use when two or more rawinsonde observations lie within the storm-influenced region. This procedure, in which the observations determine some parameters of the storm circulation itself appears capable of specifying the initial storm-track velocity about as well as present subjective practice, but removes the present SANBAR assumption of a uniform large-scale flow within the storm-influenced region. It should be especially useful when erratic tracks occur close to landfall.

Acknowledgments. We are grateful to Patricia Strat, Massachusetts Institute of Technology, for aid in tabulation and analysis of data, to Roy Jenne and Paul Mulder, National Center for Atmospheric Research, for providing data and for preparing revised SANBAR forecasts, to Isabelle Kole for preparation of the manuscript, and to Air Force Geophysics Laboratory for support under Contract F19628-75-C-0059.

REFERENCES

Adams, A. L., and F. Sanders, 1975: Application of satellite cloud-motion vectors to hurricane track prediction. Sci. Rep. No. 1, Contract F 19628-75-C0059, AFCRL-TR-75-0635.

Birchfield, G. E., 1960: Numerical prediction of hurricane movement with the use of a fine grid. *J. Meteor.*, **17**, 406–414.

Dunn, G. E., R. C. Gentry and B. M. Lewis, 1968: An eight-year experiment in improving forecasts of hurricane motion. *Mon. Wea. Rev.*, **96**, 708–713.

Hebert, P. J., 1976: Atlantic hurricane season of 1975. *Mon. Wea. Rev.*, **104**, 453–465.

Hovermale, J. B., 1975: First season storm movement characteristics of the NMC objective hurricane forecast model. Paper presented at Twelfth Annual NOAA NWS Warning Service Evaluation Conference, Coral Gables, FL.

Jordan, E. S., 1952: An observational study of the upper-wind circulation around tropical storms. *J. Meteor.*, **9**, 340–346.

Kasahara, A., 1959: A comparison between geostrophic and nongeostrophic numerical forecasts of hurricane movement with the barotropic steering model. *J. Meteor.*, **16**, 371–384.

Pike, A. C., 1972: Improved barotropic hurricane track prediction by adjustment of the initial wind field. NOAA Tech. Memo. NWS SR-66.

Riehl, H., W. H. Haggard and R. W. Sanborn, 1956: On the prediction of 24 h hurricane motion. *J. Meteor.*, **13**, 415–420.

Sanders, F., and R. W. Burpee, 1968: Experiments in barotropic hurricane track forecasting. *J. Appl. Meteor.*, **7**, 313–323.

——, A. C. Pike and J. P. Gaertner, 1975: A barotropic model for operational prediction of tracks of tropical storms. *J. Appl. Meteor.*, **14**, 265–280.

——, and N. J. B. Gordon, 1976: A study of forecast errors in an operational model for predicting paths of tropical storms. Sci. Rep. No. 2, Contract F19628-75-C-0059, AFGL-TR-77-0079.

Vanderman, L. W., 1962: An improved NWP model for forecasting the paths of tropical cyclones. *Mon. Wea. Rev.*, **90**, 19–22.